

## Lattice study of the gluon propagator in momentum space

C. Bernard

*Department of Physics, Washington University, St. Louis, Missouri 63130*

C. Parrinello

*Physics Department, New York University, 4 Washington Place, New York, New York 10003  
and Physics Department, Brookhaven National Laboratory, Upton, New York 11973*

A. Soni

*Physics Department, Brookhaven National Laboratory, Upton, New York 11973*

(Received 2 July 1993)

We consider pure glue QCD at  $\beta=5.7$ ,  $\beta=6.0$ , and  $\beta=6.3$ . We evaluate the gluon propagator both in time at zero three-momentum and in momentum space. From the former quantity we obtain evidence for a dynamically generated effective mass, which at  $\beta=6.0$  and  $\beta=6.3$  increases with the time separation of the sources, in agreement with earlier results. The momentum space propagator  $G(k)$  provides further evidence for mass generation. In particular, at  $\beta=6.0$ , for  $300 \text{ MeV} \lesssim k \lesssim 1 \text{ GeV}$ , the propagator  $G(k)$  can be fit to a continuum formula proposed by Gribov and others, which contains a mass scale  $b$ , presumably related to the hadronization mass scale. For higher momenta Gribov's model no longer provides a good fit, as  $G(k)$  tends rather to follow an inverse power law  $\approx 1/k^{2+\gamma}$ . The results at  $\beta=6.3$  are consistent with those at  $\beta=6.0$ , but only the high momentum region is accessible on this lattice. We find  $b$  in the range of 300 to 400 MeV and  $\gamma$  about 0.7. Fits to particle + ghost expressions are also possible, often resulting in low values for  $\chi^2_{\text{DF}}$ , but the parameters are very poorly determined. On the other hand, at  $\beta=5.7$  (where we can only study momenta up to 1 GeV)  $G(k)$  is best fit to a simple massive boson propagator with mass  $m$ . We argue that such a discrepancy may be related to a lack of scaling for low momenta at  $\beta=5.7$ . From our results, the study of correlation functions in momentum space looks promising, especially because the data points in Fourier space turn out to be much less correlated than in real space.

PACS number(s): 12.38.Gc

### I. INTRODUCTION

The possibility of studying nonperturbatively on the lattice gauge-dependent quantities provides in principle a unique tool to test QCD at the level of the basic fields entering the continuum Lagrangian. From this point of view, the gluon propagator in the pure glue theory is perhaps the simplest quantity. From its study one expects to obtain among other things a better understanding of the infrared behavior of the theory and of the mechanism of gluon confinement. As a result we may also hope to acquire a better understanding of the hadronization phenomena and of the glueball spectrum [1].

Let us first review what is known from perturbation theory: consider the expression (in Minkowski space-time)

$$D_{\mu\nu}^{ab}(k) \equiv -i \int d^4x \langle 0 | T [ A_\mu^a(x) A_\nu^b(0) ] | 0 \rangle e^{ik \cdot x} . \quad (1)$$

From the Faddeev-Popov quantization in a class of covariant gauges one gets the simple Slavnov identity

$$k^\mu k^\nu D_{\mu\nu}^{ab}(k) = -i\alpha \delta^{ab} , \quad (2)$$

where  $\alpha$  is the gauge parameter. From Lorentz covariance, the general solution to (2) can be written as

$$D_{\mu\nu}^{ab}(k) = -i\delta^{ab} \left[ \left( g_{\mu\nu} - \frac{k_\mu k_\nu}{k^2} \right) \frac{1}{1 + \Pi(k^2, \alpha)} + \alpha \frac{k_\mu k_\nu}{k^2} \right] \frac{1}{k^2} . \quad (3)$$

Equation (2) implies that the longitudinal part of the propagator gets trivially renormalized, so that the vacuum polarization  $\Pi(k^2, \alpha)$  just renormalizes the transverse propagator. The renormalization constant  $Z_3$  for the gauge fields,  $A_i = Z_3^{1/2} A_i^R$ , is defined as

$$Z_3^{-1} = 1 + \Pi \left( \frac{\Lambda}{\mu}, \alpha \right) , \quad (4)$$

where  $\Lambda$  is an ultraviolet cutoff and  $k^2 = -\mu^2$  is a space-like value of the momentum. In general  $Z_3$  is gauge dependent.

One can then rewrite the unrenormalized transverse gluon propagator as

$$D_{\mu\nu}^{T ab}(k^2) \Big|_{k^2 = -\mu^2} = \frac{i}{\mu^2} Z_3 \left[ g_{\mu\nu} + \frac{k_\mu k_\nu}{\mu^2} \right] \delta^{ab} . \quad (5)$$

Unlike QED, in QCD we know from the properties of the  $\beta$  function that perturbation theory can only be ap-

plied to the study of the large- $k^2$  behavior of Green's functions. In such a region one gets, at the one-loop level [2],

$$Z_3 = 1 + \frac{g^2}{16\pi^2} \left[ \frac{13}{3} - \alpha \right] 3 \ln \left[ \frac{\Lambda}{\mu} \right]. \quad (6)$$

In general, at each order in  $g^2$  perturbative corrections depend logarithmically on  $k$ , so that in the deep Euclidean region ( $k^2 \rightarrow \infty$ ) gluon propagators behave essentially in the same way as the photon propagators, as long as one considers a finite order in perturbation theory.

In the infrared region things are probably different. In fact, in the simpler QED case perturbation theory is still reliable, and one can evaluate order by order the vacuum polarization function. In particular, one finds that  $\Pi^{\text{QED}}(k^2=0)$  is finite if all the fermions are massive (we omit from now on the explicit  $\alpha$  dependence of vacuum polarization functions). This implies that the  $k^2=0$  pole of the free photon propagator is still present after radiative corrections are taken into account, so that the photon remains a massless particle. Such corrections only affect the residue at the pole, resulting in charge renormalization.

On the other hand, consider QCD without quarks. The corresponding Lagrangian does not contain any mass scale in four dimensions, yet if the theory is confining a mass scale must be dynamically generated in some way, since the confinement potential  $V(r) = Kr$  contains such a scale. Such a mass  $M$  cannot be generated in perturbation theory, since it must satisfy

$$M(g, \mu) = \mu \exp \left[ - \int^g \frac{dg'}{\beta(g')} \right], \quad (7)$$

where  $\mu$  is a renormalization scale  $\mu$ . For small  $g$ , one has

$$M(g, \mu) \approx \mu \exp \left[ - \frac{\text{const}}{g^2} \right] \quad \text{when } g \rightarrow 0 \quad (8)$$

so that  $M(g)$  has an essential singularity at  $g=0$ .

Such a mass scale may show up in the vacuum polarization function for the gluon. Indeed, while contributions to  $\Pi(k^2)$  proportional to finite powers of  $g$  have for large  $k^2$  a logarithmic momentum dependence, nonperturbative effects may generate terms in  $\Pi(k^2)$  proportional to *negative* powers of the squared four-momentum: for instance,

$$\Pi(k^2) = - \frac{m^2(g, \mu)}{k^2} + \frac{b^4(g, \mu)}{k^4} + O(g^2), \quad (9)$$

where  $m(g, \mu)$ ,  $b(g, \mu)$  have the dimension of a mass and depend nonanalytically on  $g$ . For example, the case  $b=0$ ,  $m \neq 0$  gives rise to a mass pole in the gluon propagator and corresponds to the standard Schwinger mechanism [3].

In the above formula  $O(g^2)$  denotes contributions which can be represented as a power series in  $g^2$ . Such series, when truncated to a finite order in  $g^2$ , behave like polynomials in  $\ln(k^2/\mu^2)$  for large  $k^2$ . On the other hand, the sum of the contributions to all orders in  $g^2$  can

generate an anomalous dimension  $\gamma$  [4]; in such a case for  $k^2 \rightarrow \infty$  the propagator behaves like  $1/k^{2+\gamma}$ . The nonperturbative behavior of the Euclidean gluon propagator has been investigated in the continuum by many authors with different methods and in different gauges [5–10]. In some of these attempts a very singular gluon propagator was found, behaving like  $k^{-4}$  in the limit  $k^2 \rightarrow 0$  [10], and a confining property was inferred from such behavior. On the other hand, other work points towards the elimination at the nonperturbative level of the singularity at  $k^2=0$  of the propagator [6,7,9], as a consequence of dynamical mass generation.

In particular, a very peculiar momentum dependence, consistent with the above scenario, has been predicted as arising from a modification of the standard path integral Faddeev-Popov formula in the Landau gauge by the introduction of a nonperturbative gauge-fixing procedure [5,8]. Such improved implementation of the Landau gauge is expressed by the equations

$$\partial \cdot A = 0 \quad \text{and} \quad X_{\text{FP}}[A] > 0, \quad (10)$$

where  $X_{\text{FP}}[A]$  is the Faddeev-Popov operator in the Landau gauge, which in general is not positive definite. The positivity requirement in (10) can be seen as a recipe to get rid (although not completely [11]) of Gribov copies [5]. In the gauge (10), the (transverse) gluon propagator in momentum space has been argued to be of the form [5,8]

$$G(k) \approx \frac{k^2}{k^4 + b^4}, \quad (11)$$

where  $b$  is a dynamically generated mass scale. Equation (11) corresponds to the case  $m=0, b \neq 0$  in (9). It implies that in the continuum

$$G(\mathbf{k}=0, t) \approx e^{-(b/\sqrt{2})t} \left[ \cos \left[ \frac{b}{\sqrt{2}} t \right] - \sin \left[ \frac{b}{\sqrt{2}} t \right] \right]. \quad (12)$$

Remarkably, the same predictions were also obtained in the study of Schwinger-Dyson equations [7].

The above expression lends itself to intriguing speculations: the absence of any particle singularity on the real  $k^2$  axis predicts the absence of an asymptotic gluon state. It may describe a short-lived excitation, giving rise to a gluon jet. In this framework, the mass scale  $b$  appearing in the above formulas may perhaps be interpreted as a hadronization scale.

The lattice gluon field can be defined as [12]

$$A_\mu(n) \equiv \frac{U_\mu(n) - U_\mu^\dagger(n)}{2ia} - \frac{1}{3} \text{Tr} \left[ \frac{U_\mu(n) - U_\mu^\dagger(n)}{2ia} \right], \quad (13)$$

where  $a$  is the lattice spacing. Thus the lattice gluon propagator in  $x$  space is the expectation value of

$$G_{\mu\nu}(x, y) \equiv \text{Tr} [ A_\mu(x) A_\nu(y) ]. \quad (14)$$

An important point is that on the lattice one can define and implement the analogue of the gauge condition (10).

In fact, given any link configuration  $\{U\}$ , one can define a function of the gauge transformations  $g$  on  $\{U\}$ :

$$F_U[g] \equiv -\frac{1}{V} \sum_{n,\mu} \text{Re Tr} [U_\mu^g(n) + U_\mu^{g^\dagger}(n - \hat{\mu})], \quad (15)$$

where  $V$  is the lattice volume and  $U^g$  indicates the gauge-transformed link  $U_\mu^g(n) \equiv g(n)U_\mu(n)g^\dagger(n + \hat{\mu})$ . An iterative minimization of  $F_U[g]$  obtained by performing suitable gauge transformations generates a configuration  $\{U^{\bar{g}}\}$  which satisfies the lattice version of (10), defined in terms of a lattice Faddeev-Popov operator [13]. This is just the Hessian matrix associated with  $F_U[g]$ , that is,  $\delta^2 F_U[g]/\delta g_1 \delta g_2$ . As we have already mentioned for the continuum, such a gauge is not completely free of Gribov copies. This is also true on the lattice, and corresponds to the fact that for a fixed configuration  $\{U\}$  the function (15) may have several local minima (see, for example [14]).

In general, Zwanziger [13] showed that on the lattice one has qualitatively the same scenario for the Landau gauge as in the continuum. Indeed, there exists a bounded region  $\Omega$ , defined by the positivity requirement for the lattice Faddeev-Popov operator, which satisfies bounds analogous to the ones derived for the continuum model. Considering then a restriction of the functional integration to the region  $\Omega$ , Zwanziger was able to obtain predictions for the lattice gluon propagator consistent with the continuum ones given in (11) and (12).

At this point it is natural to try and test numerically predictions such as (11) and (12).

Numerical studies have been performed in the past years for the zero spatial momentum Fourier transform of (14), namely  $G(\mathbf{k}=0, t) \equiv \sum_{i=1}^3 G_{ii}(\mathbf{k}=0, t)$  [12,15,16]. These studies reported evidence of an effective gluon mass that increases with the time separation for short time intervals. This feature, which would be unacceptable for the propagator of a real physical particle since it violates the Källén-Lehmann representation, is in qualitative agreement with the continuum prediction (12) and may be in principle acceptable for a confined particle [7,12]. Another lattice approach to the gluon mass was given in [17].

Our work aims to test at a more quantitative level continuum predictions and to extend the above results through the study of the gluon propagator at nonzero momenta.

## II. NUMERICAL RESULTS

We study pure glue QCD on  $16^3 \times 40$  and  $24^3 \times 40$  lattices at  $\beta=6.0$ , on a  $24^4$  lattice at  $\beta=6.3$ , and on a  $16^3 \times 24$  lattice at  $\beta=5.7$ .

### A. Technical remarks

It is worth remarking that, unlike simulations involving quenched quark propagators, evaluations of purely gluonic correlation functions can take full advantage of the translational symmetry of the theory in order to improve statistics. On the other hand, such quantities turn out to be very sensitive to the numerical accuracy of

gauge fixing. Empirically, at  $\beta=6.0$  and  $\beta=6.3$  we find that when the minimization of  $F_U[g]$  has reached an accuracy such that in  $\sim 50$  iterations  $F_U[g]$  changes less than  $\approx 0.05\%$ , then the signal for the propagators is sufficiently stable against additional gauge fixing. In other words, the variation in each data point for the propagator arising from additional gauge fixing is typically much smaller than the final error bar associated to the data point. On the contrary, we will see that at  $\beta=5.7$  our stability requirement for  $F_U[g]$  does not suffice to guarantee a completely stable propagator.

Even at  $\beta=6.0$  and  $\beta=6.3$ , though, when our empirical criterion gets satisfied the system has not yet reached complete equilibrium, in spite of the fact that such an accuracy is roughly one order of magnitude better than the typical one adopted in simulations of hadron phenomenology. This can be seen by performing the following test [12]: in the Landau gauge  $\partial_\mu A_\mu = 0$  it follows from the periodic boundary conditions that

$$A_0(t) \equiv \sum_{\vec{x}} A_0(\vec{x}, t) \quad (16)$$

should not depend on  $t$ . In lattice language, this means that once the Landau gauge has been numerically implemented in a configuration, then the sum over the sites in a fixed time slice of the time component of the gauge field should be the same on each time slice. In Fig. 1 we plot one of the diagonal elements of the matrix  $A_0(t)$  as a function of  $t$  for one of our gauge-fixed configurations on the  $16^3 \times 40$  lattice at  $\beta=6.0$ . This test shows that even when the accuracy of our numerical gauge fixing is sufficient for the gluon propagator, there are other quantities for which the gauge fixing need not be adequate. As a consequence, it would be dangerous in a calculation to rely on some standard *a priori* criterion when estimating the required precision for the gauge fixing, since such precision strongly depends on the specific observable under consideration. We remark that the gauge-fixing test provided by  $A_0(t)$  is in fact more stringent than the one used in [12].

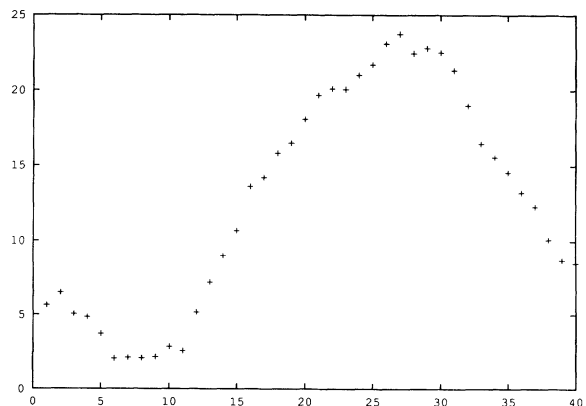


FIG. 1.  $A_0(t)$  vs  $t$  for one gauge-fixed configuration on the  $16^3 \times 40$  lattice at  $\beta=6.0$ .

### B. Results at $\beta=6.0$ and $\beta=6.3$

Here we give results for a set of 25 configurations of size  $16^3 \times 40$  at  $\beta=6.0$ , a set of 8 configurations of size  $24^3 \times 40$  at  $\beta=6.0$ , and finally a set of 20 configurations of size  $24^4$  at  $\beta=6.3$ .

As a first step we have evaluated  $G(\mathbf{k}=0, t)$ ; our results confirm that this propagator exhibits a massive decay in time, with an effective mass  $am(t) \equiv \ln[G(\mathbf{k}=0, t)/G(\mathbf{k}=0, t+a)]$  that increases with  $t$  for short times. In Fig. 2 we plot  $am(t)$  versus  $t$  with jackknife errors [18] on the  $16^3 \times 40$  lattice. Assuming the value of the inverse lattice spacing  $a^{-1}=2.1$  GeV at  $\beta=6.0$  [19], the effective gluon mass  $m(t)$  ranges approximately between 220 and 870 MeV. A similar behavior is observed for the  $24^3 \times 40$  lattice, with the effective mass ranging between 240 and 1200 MeV.

At this point we have attempted to fit  $G(\mathbf{k}=0, t)$  to the continuum form (12) and to the form commonly referred to as particle + ghost, that is

$$G(\mathbf{k}=0, t) = C_1 \exp(-M_1 t) + C_2 \exp(-M_2 t), \quad (17)$$

where  $C_2$  is constrained to be negative.

As is well known, the data points obtained from a Monte Carlo simulation are in general statistically correlated; in the present case, the correlated data are the values of the propagator  $G(\mathbf{k}=0, t)$  at different time slices. For this reason, one should perform  $\chi^2$  fits by using the definition of  $\chi^2$  which involves the full covariance matrix [20].

By inspection of the covariance matrix for  $G(\mathbf{k}=0, t)$ , it turns out that the off-diagonal matrix elements are typically of the same size as the diagonal ones, which means that our data points are highly correlated in  $t$ . Consequently,  $\chi^2$  fits are not well controlled because the covariance matrix is nearly singular. Much higher statistics would be required to get well-behaved fits.

As it is not possible in this case to make fits using the full covariance matrix, we are forced to use the naive definition of  $\chi^2$ , where the data points are simply weighted by their standard error bar. Of course, in such an approach  $\chi^2$  has no simple relation to "goodness of fit."

In this approximation, it turns out that Gribov's for-

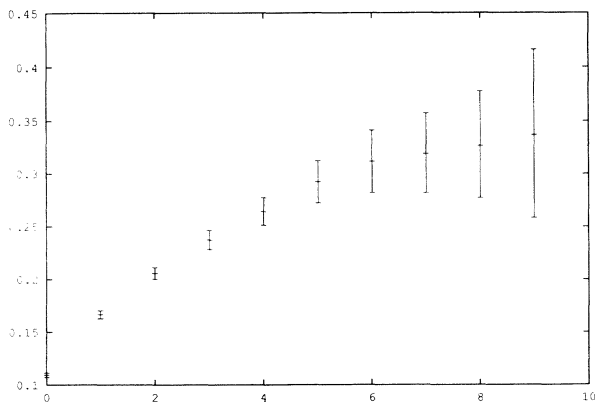


FIG. 2. Effective gluon mass in lattice units vs  $t$  on the  $16^3 \times 40$  lattice at  $\beta=6.0$ .

mula, i.e., Eq. (11), provides, for small  $t$ , a good fit to  $G(\mathbf{k}=0, t)$ , better than the one obtained from the particle + ghost expression. In fact, although  $\chi_{\text{DF}}^2$  is not a reliable indicator of the goodness of a fit when the covariance matrix is not taken into account, nonetheless the relative  $\chi_{\text{DF}}^2$  of two fits provides some indication of which fit is better. On the  $16^3 \times 40$  lattice at  $\beta=6.0$ , the lowest value for  $\chi_{\text{DF}}^2$  obtained from a fit to Gribov's formula is  $\chi_{\text{DF}}^2=0.18$ , while from the four-parameter fit to particle + ghost one gets  $\chi_{\text{DF}}^2=0.34$ . Moreover, the latter kind of fit is much less stable against varying the initial guess for the fit parameters; i.e., many local minima for  $\chi^2$  can be found. Using  $a^{-1}=2.1$  GeV, we obtain for the  $b$  parameter in (12)  $b=237 \pm 7$  MeV,  $\chi_{\text{DF}}^2=0.18$ , where the error in  $b$  is a jackknife one. Of course one does not get good agreement by using a conventional four-parameter double exponential form, that is if one constrains  $C_2$  in (17) to take positive values. Indeed, in this case the effective mass would always decrease with  $t$ , in contrast with what is observed.

The statistical difficulties mentioned above forbid a complete analysis of  $G(\mathbf{k}=0, t)$ ; in particular, we cannot effectively study the large- $t$  region, where according to (12) the propagator may become negative and then oscillate.

Our analysis of the momentum space propagator  $G(k) \equiv \sum_{\mu=1}^4 G_{\mu\mu}(k)$  does not have the same statistical difficulties as in the case of  $G(\mathbf{k}=0, t)$ . This quantity is obtained by performing explicitly the lattice Fourier transform of the propagator (14).

In fact, the covariance matrix associated with  $G(k)$  turns out to be much more "diagonal" than the one for  $G(\mathbf{k}=0, t)$ ; in other words, the data points are much less correlated in momentum space than they are in  $t$ . We find that  $G(k)$  is very well determined in a significant interval of physical momenta up to  $k \approx 2$  GeV, which is in fact roughly the value of the ultraviolet cutoff  $a^{-1}$  (see Fig. 3). As a consequence we have been able to obtain good fits to  $G(k)$  taking into account correlations. Figure 3 also shows that the data points from the two lattices at  $\beta=6.0$  are in good agreement over most of the momentum range.

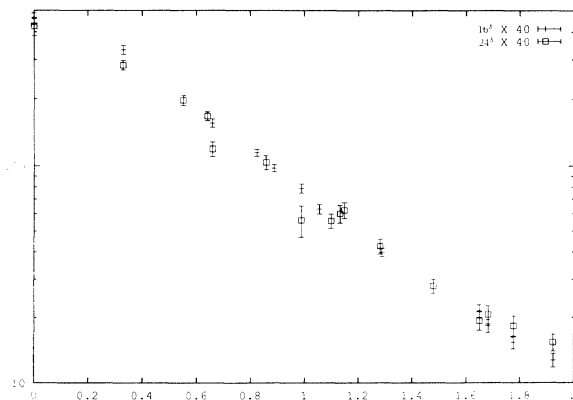


FIG. 3. Momentum space propagator vs  $k$  in GeV on the  $16^3 \times 40$  and  $24^3 \times 40$  lattices at  $\beta=6.0$ . We assume  $a^{-1}=2.1$  GeV.

At this point we attempt to fit  $G(k)$  to the continuum formula (11) and, for a comparison, to a standard massive propagator  $G_{\text{mass}}(k) = A/(k^2 + m^2)$ . The fits are performed including in  $\chi^2$  the covariance matrix. Consider first the  $16^3 \times 40$  lattice: it turns out that for momenta between  $\approx 300$  MeV and  $\approx 1$  GeV formula (11) fits the data well (see Fig. 4). Indeed, for such a fit we obtain  $\chi_{\text{DF}}^2 = 1.3$  and  $b = 341 \pm 12$  MeV, assuming  $a^{-1} = 2.1$  GeV. The error is given in terms of the parameter covariance matrix [20], and we are not including the uncertainty in the value of  $a^{-1}$ .

We compare this result to the best fit that one can obtain from the standard massive propagator, for which we obtain<sup>1</sup>  $\chi_{\text{DF}}^2 = 2.9$ .

On the other hand, in the range of momenta 1–2 GeV the formula (11) and the massive propagator expression fit the data very poorly, resulting in  $\chi_{\text{DF}}^2 > 10$ . A good fit in this range is obtained by assuming an inverse power law behavior  $G(k) = A/k^{2+\gamma}$  (see Fig. 5). We obtain  $\gamma = 0.7 \pm 0.2$ ,  $\chi_{\text{DF}}^2 = 1$ . The fact that (11) does not fit the high momentum region well presumably explains the discrepancy between the value of  $b$  obtained from  $G(k)$  at low momenta and that obtained from  $G(\mathbf{k}=0, t)$ , which depends on the complete range of momenta.

The situation is qualitatively similar on the  $24^3 \times 40$  lattice. However, presumably due to the lower statistics, there is clear dispersion in the data (see Fig. 3), which means that no fit will be particularly good. In fact, up to 1 GeV the best fit is given by (11) (see Fig. 4), and we obtain  $b = 333 \pm 12$  MeV,  $\chi_{\text{DF}}^2 = 5.8$ . Between 1 and 2 GeV we are unable to perform fits with the covariance matrix, due to the poor statistics. Without the covariance matrix, an inverse power law with  $\gamma \approx 0.6$  again reproduces the data well (see Fig. 5).

Summarizing, the data for  $G(k)$  at  $\beta = 6.0$  on the

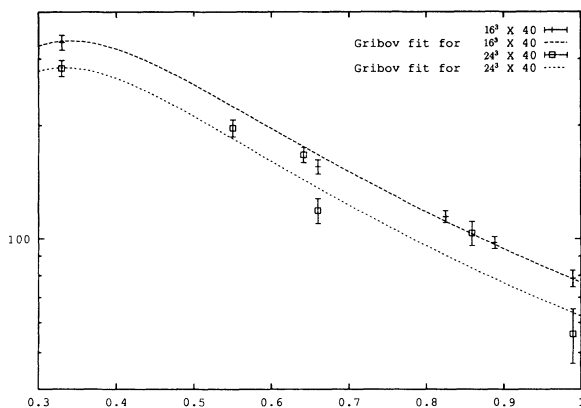


FIG. 4.  $G(k)$  vs  $k$  in GeV and fit to the form (11) on the  $16^3 \times 40$  and  $24^3 \times 40$  lattices at  $\beta = 6.0$ .

<sup>1</sup>We have also attempted a fit to a form proposed in [6]. Such a form in the low momentum region is very similar to a standard massive propagator. The standard massive form appears to provide a better fit.

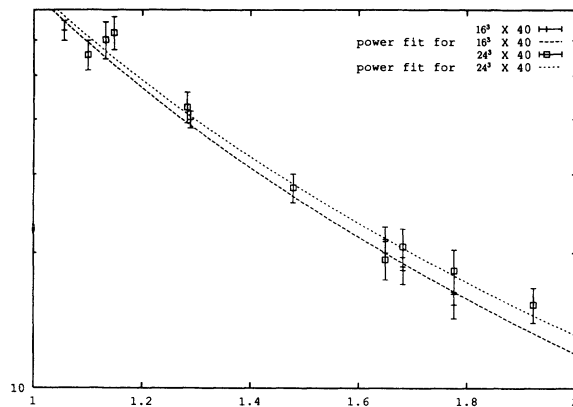


FIG. 5.  $G(k)$  vs  $k$  in GeV and fit to an inverse power law on the  $16^3 \times 40$  and  $24^3 \times 40$  lattices at  $\beta = 6.0$ . In the latter case, the covariance matrix is not included in the fit.

$16^3 \times 40$  lattice up to momenta of order 1 GeV prefer somewhat formula (11), which describes the mass generation in the manner of Gribov, over a standard massive propagator. In the momentum range 1–2 GeV the propagator is best reproduced by the inverse power law behavior  $G(k) \approx 1/k^{2+\gamma}$ , where  $\gamma$  could be interpreted as the anomalous dimension of  $G(k)$ . Indeed, our results in such a region could also be sensitive to the lattice ultraviolet cutoff  $a^{-1}$ . The fact that the  $\beta = 6.3$  results (described below) agree with those at  $\beta = 6.0$  gives some indication that such cutoff effects are not overwhelmingly large. An additional test for lattice artifacts is described at the end of the next section.

On the other hand, the results from the  $24^3 \times 40$  lattice, due to the poor statistics, do not provide by themselves a strong confirmation of the above picture. Still, in the low momentum region the Gribov fit works better than a standard massive one and gives a value for  $b$  which is consistent with the one from the  $16^3 \times 40$  lattice, but we get a high value for  $\chi_{\text{DF}}^2$ . Moreover, in the higher momentum region we are unable to use the covariance matrix.

We consider now a set of 20 configurations on a  $24^4$  lattice at  $\beta = 6.3$ .

Starting again from the evaluation of  $G(\mathbf{k}=0, t)$ , we give in Fig. 6 the effective gluon mass with jackknife errors. Again, the effective mass  $am(t)$  appears to increase with  $t$ . Assuming  $a^{-1} = 3.2$  GeV at  $\beta = 6.3$  [19],  $m(t)$  ranges approximately between 200 and 670 MeV.

It turns out that we have the same statistics problem as at  $\beta = 6.0$ : The data for  $G(\mathbf{k}=0, t)$  are highly correlated in  $t$ , so that it is impractical to make fits using the full covariance matrix.

Next we consider the propagator  $G(k)$  in momentum space. We again find that correlations between different values of  $k$  are much smaller than the correlations in  $t$ , so that the covariance matrix is now well behaved. The best fit to  $G(k)$  is obtained from the inverse power law  $G(k) = A/k^{2+\gamma}$  (see Fig. 7). We assume  $a^{-1} = 3.2$  GeV [19] and get  $\gamma = 0.68 \pm 0.08$ ,  $\chi_{\text{DF}}^2 = 1.9$ .

Given the momentum range of such a fit, which starts around 1 GeV and goes up to momenta of the order  $a^{-1}$ ,

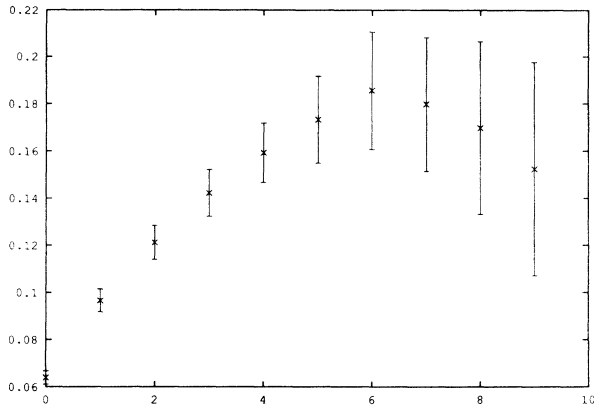


FIG. 6. Effective gluon mass in lattice units vs  $t$  at  $\beta=6.3$ .

such a result is quite consistent with the behavior observed at  $\beta=6.0$ . In particular, the value for  $\gamma$  agrees with the one obtained on the  $16^3 \times 40$  lattice.

Both at  $\beta=6.0$  and  $\beta=6.3$  we have also attempted four-parameter fits, in terms of the particle + ghost form  $G(k) = A/(k^2 + m_1^2) + B/(k^2 + m_2^2)$ , with  $A > 0$  and  $B < 0$ . Although low values of  $\chi_{DF}^2$  can sometimes be obtained, the determination of the fit parameters is very poor.

### C. Results at $\beta=5.7$ and comparison of lattices

Here we give results for a set of 16 configurations on a  $16^3 \times 24$  lattice at  $\beta=5.7$ . After implementing our standard level of gauge fixing, we find that the data for  $G(k=0, t)$  are, as usual, not suitable for  $\chi^2$  fits with the full covariance matrix. When fit without the covariance matrix, the data seem to be best reproduced by a simple decreasing exponential, unlike what happened on the other data sets at weaker couplings. Correspondingly, there is no clear evidence for an increase of the effective gluon mass  $am(t)$  on a significant time interval (see Fig. 8).

In addition, the results for  $G(k)$  on this lattice differ from what we observed at weaker couplings. Assuming  $a^{-1} = 1.2$  GeV, our data for  $G(k)$  cover a momentum

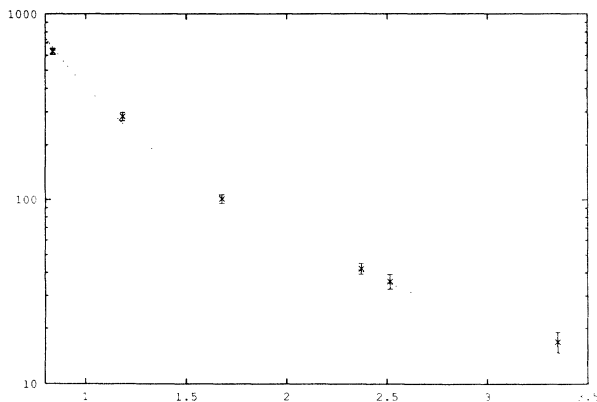


FIG. 7. The best fit of  $G(k)$  vs  $k$  in GeV to an inverse power law (solid line) on the  $24^4$  lattice at  $\beta=6.3$ .

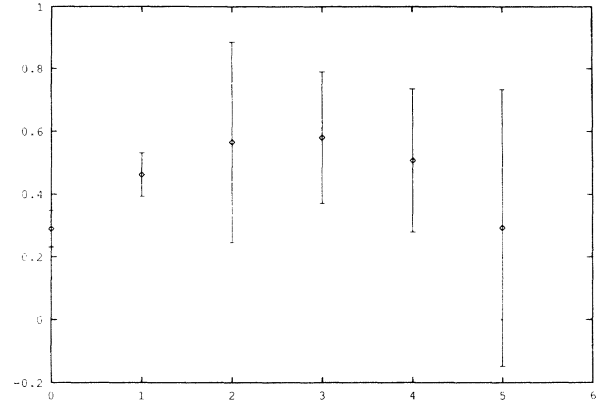


FIG. 8. Effective gluon mass in lattice units vs  $t$  on the  $16^3 \times 24$  lattice at  $\beta=5.7$ .

range up to roughly 1 GeV. The best fit to such data (including the full covariance matrix) is provided by a free massive boson propagator  $G(k) \approx 1/(k^2 + m^2)$ . We obtain  $m = 590 \pm 30$  MeV, with  $\chi_{DF}^2 = 1.4$ .

Since from the above analysis the results at  $\beta=5.7$  seem to differ significantly from those at  $\beta=6.0$  and  $\beta=6.3$ , we have investigated the effect of improving the accuracy of the gauge fixing. After 300 additional sweeps on each configuration, we repeat our measurements.

For  $G(k=0, t)$  it turns out that while the central values of the individual data points do change significantly, the pattern of the effective mass  $am(t)$  is basically the same. Not surprisingly, the best fit is still provided by a simple exponential, with a value for the mass parameter which is close to the one obtained before the additional sweeps; in other words, to a first approximation the effect of additional gauge fixing has been a rescaling of the data points. As far as  $G(k)$  is concerned, the individual data points are not much affected by the additional gauge fixing. In fact, the best fit to the data is still provided by a free massive boson, but now we obtain  $m = 630 \pm 40$  MeV, with  $\chi_{DF}^2 = 3.3$ . Moreover, the error bars of some data points have become slightly bigger (see Fig. 9).

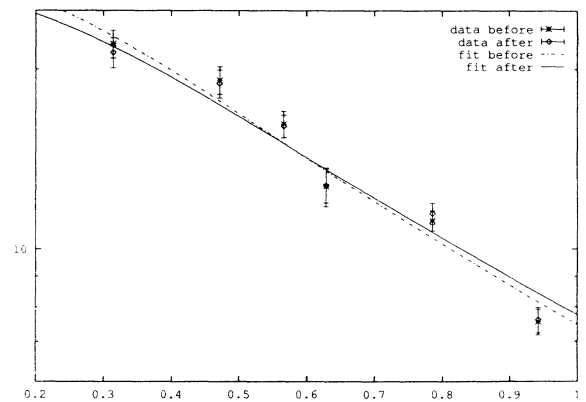


FIG. 9.  $G(k)$  vs  $k$  in GeV and fit to a massive boson propagator before and after additional gauge fixing on the  $16^3 \times 24$  lattice at  $\beta=5.7$ .

Summarizing, we find that the qualitative behavior of the data is not changed by the additional gauge fixing, maintaining the discrepancy with the other lattices. However, since the value of  $\chi_{DF}^2$  in the fit for  $G(k)$  has increased as well as some individual error bars for the data points, the additional gauge fixing seems to have increased the “noise” in the evaluation of  $G(k)$ . This may be related to the existence of Gribov copies in our gauge [21].

To go back to the main issue, which is the discrepancy between  $G(k)$  at  $\beta=5.7$  and at weaker couplings, our present data give some indication that such a discrepancy may be due to a lack of scaling at  $\beta=5.7$ . To illustrate this point we have plotted for each data set the quantity  $100 \times G(k)/G(k=0)$ . Such a quantity should not depend on  $\beta$ , as long as one is in the scaling region. On the other hand, when comparing  $G(k)/G(k=0)$  at different  $\beta$  one has an uncertainty related to the determination of the horizontal scale, i.e., the scale of physical momenta, depending on the values of  $a^{-1}$ . With this caveat in mind, we show in Figs. 10 and 11 the quantity  $100 \times G(k)/G(k=0)$  as obtained from our different data sets. (For the lattice at  $\beta=5.7$  we use the data after the additional gauge fixing.) We again assume  $a^{-1}=1.2$  GeV at  $\beta=5.7$ ,  $a^{-1}=2.1$  GeV at  $\beta=6.0$ , and  $a^{-1}=3.2$  GeV at  $\beta=6.3$ .

From the above-mentioned figures it turns out that in general the data agree well, but significant deviations are observed in the low momentum region; in particular, the data at  $\beta=5.7$  for momenta up to  $\approx 650$  MeV are rather different from the corresponding data at  $\beta=6.0$  (see Fig. 10). This may account for the observed discrepancies, although further analysis and better statistics are needed to clarify this issue.

At this point it is worth mentioning that we have checked the stability of our fits for  $G(k)$  versus the use of continuum and lattice formulas. In fact, especially when the data points correspond to lattice momenta of order  $a^{-1}$ , one may wonder whether more accurate fits could be obtained by using lattice versions of our formulas. One can devise such expressions by substituting  $k^2$  with  $2/a^2 \sum_{\mu} [1 - \cos(k_{\mu} a)]$  in the continuum ones.

We have also checked the stability of the results under

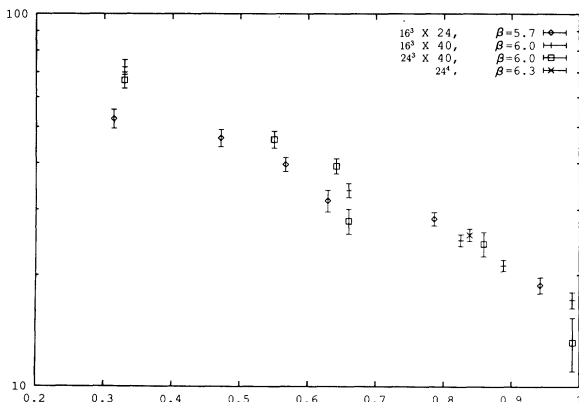


FIG. 10.  $100 \times G(k)/G(k=0)$  on the different lattices (low momentum region).

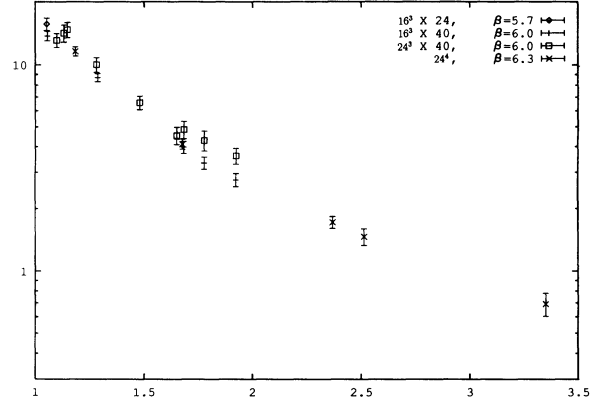


FIG. 11. Same as Fig. 10, in a higher momentum region.

change from covariant to noncovariant fits. It turns out that when the covariance matrix is well behaved, which is what typically happens on our lattices for  $G(k)$ , the fit is not very sensitive to the different definitions for  $\chi^2$ . Moreover, the fits are not sensitive to the difference between continuum and lattice formulas, not even in the higher momentum region. This is shown in Fig. 12 for the  $24^4$  lattice at  $\beta=6.3$ , where we compare lattice and continuum versions of the best fit to an inverse power law, with and without the full covariance matrix.

One gets from the fit to the lattice formula, without covariance matrix,  $\gamma \approx 0.69$ , and from the fit to the continuum formula, without the covariance matrix,  $\gamma \approx 0.61$ . These numbers should be compared to  $\gamma = 0.68 \pm 0.08$ , which is the result we obtained from the fit to the continuum power law which included the full covariance matrix.

### III. CONCLUSIONS

Let us summarize our results.

We have evaluated  $G(\mathbf{k}=0, t)$  and  $G(k)$  on four different lattices at three different values of  $\beta$ . All the data provide evidence for dynamical mass generation, in agreement with previous results for  $G(\mathbf{k}=0, t)$ .

(1) For  $G(\mathbf{k}=0, t)$  the data at  $\beta=6.0$  and  $\beta=6.3$  show

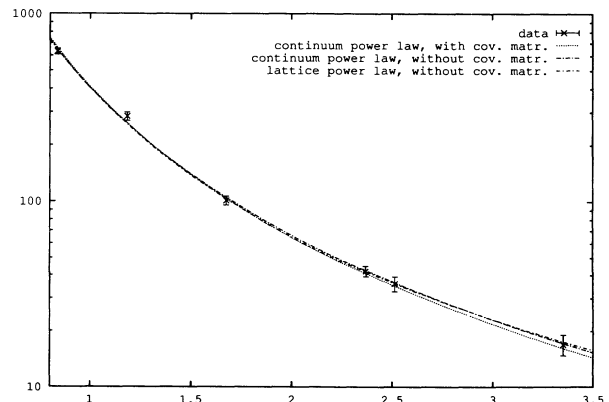


FIG. 12.  $G(k)$  vs  $k$  in GeV on the  $24^4$  lattice at  $\beta=6.3$  and the best fits to an inverse power law.

an effective gluon mass which increases with the time separation, for short times, in agreement with previous results. At  $\beta=5.7$  there is no clear signal for an increasing effective mass over more than 1 time slice. A more detailed analysis of  $G(\mathbf{k}=0, t)$  is not possible, due to statistical difficulties.

(2) The most interesting quantity is the momentum space propagator  $G(k)$ , which we have evaluated for the first time. It is characterized by a clear numerical signal; in particular, it turns out that the data in momentum space are much less correlated than in real space. At  $\beta=6.0$  the propagator  $G(k)$  up to momenta  $\approx 1$  GeV can best be described by the dynamical mass generation mechanism in the manner of Gribov; however, a description by a standard massive propagator is not ruled out. At higher momenta the propagator is best described by an inverse power law, which could be interpreted in terms of an anomalous dimension. The results at  $\beta=6.3$  are consistent, but only the high momentum region is accessible because of the small physical size of the lattice. Thus the behavior of the propagator for the above values of  $\beta$  could be summarized by the determination of a mass scale  $b$  and an anomalous dimension  $\gamma$ . In spite of the uncertainties in the determination of  $a^{-1}$ , our numerical values for  $\gamma$  are consistent between  $\beta=6.0$  and  $\beta=6.3$  lattices, when assuming  $a^{-1}=2.1$  GeV at  $\beta=6.0$  and  $a^{-1}=3.2$  GeV at  $\beta=6.3$ . For  $b$ , the results are consistent between the two different volumes at  $\beta=6.0$ , which are the only lattices on which it is determined.

On the other hand, at  $\beta=5.7$   $G(k)$  is best fit, up to momenta  $\approx 1$  GeV, by a simple massive propagator. We argue that such a discrepancy may be related to a lack of scaling between  $\beta=5.7$  and 6.0 for  $G(k)$  at low momenta.

In some cases, four-parameter fits to particle + ghost expressions for  $G(k)$  result in small values of  $\chi^2_{DF}$ , but as the parameters are typically very poorly determined,

such fits are not very illuminating.

In conclusion, the lattice study of gluon correlation functions, in the gauge-fixed framework which we have discussed, appears to be technically possible, although challenging. In particular, the feasibility of the study in momentum space is very promising for future applications.

A very careful analysis of systematic lattice effects and statistical errors is necessary. At the same time, a study of the gauge dependence of the mass scales related to the propagator is also in order.

*Note added.* After this paper was submitted we received a paper by Zwanziger [22] in which he makes an interesting observation regarding our Fig. 3. He notices that  $G(k=0)$  seems to have the same numerical value on our two lattices at  $\beta=6.0$ . He suggests that the apparent volume independence indicates that  $G(k=0)$  goes to a constant at infinite volume.

#### ACKNOWLEDGMENTS

C.P. wishes to thank D. Zwanziger for many illuminating discussions, Y. Shen for an interesting conversation, and the Physics Department of the University of Rome "La Sapienza" for hospitality during some stages of the present work. In particular, C.P. wants to thank G. Martinelli, N. Stella, and M. Testa for communicating to him some preliminary results and fits for the gluon propagator, obtained by their collaboration, and for a useful discussion. C.B. was partially supported by the DOE under Grant No. DE2FG02-91ER40628, and C.P. and A.S. were partially supported under U.S. DOE Contract No. DE-AC02-76CH00016. C.P. also acknowledges financial support from C.N.R. The computing for this project was done at the National Energy Research Supercomputer Center in part under the "Grand Challenge" program and at the San Diego Supercomputer Center.

- 
- [1] See, for example, J. M. Cornwall and A. Soni, *Phys. Lett.* **120B**, 431 (1983).
- [2] See, for example, T. P. Cheng and L. F. Li, *Gauge Theory of Elementary Particle Physics* (Oxford University Press, New York, 1984), p. 285.
- [3] For a review, see W. Marciano and H. Pagels, *Phys. Rep.* **C36**, 137 (1978), and references therein.
- [4] See, for example, Ref. [2], pp. 73–74.
- [5] V. N. Gribov, *Nucl. Phys.* **B139**, 1 (1978).
- [6] J. M. Cornwall, *Phys. Rev. D* **26**, 1453 (1982), and references therein.
- [7] M. Stingl, *Phys. Rev. D* **34**, 3863 (1986); U. Habel *et al.*, *Z. Phys. A* **336**, 435 (1990).
- [8] D. Zwanziger, *Nucl. Phys.* **B378**, 525 (1992).
- [9] J. M. Namyslowski, invited talk at the First German-Polish Symposium on Particles and Fields, Rydzyna, 1992 (unpublished).
- [10] S. Mandelstam, *Phys. Rev. D* **20**, 3223 (1979); M. Baker, J. S. Ball, and F. Zachariassen, *Nucl. Phys.* **B186**, 531 (1981); **B186**, 560 (1981).
- [11] M. A. Semenov-Tyan-Shanskii and V. A. Franke, in the *Proceedings of the 1982 Seminars of the Leningrad Mathematical Institute*, (Plenum, New York, 1986). Some of the results in that paper have been sharpened: see, for example, G. Dell'Antonio and D. Zwanziger, in *Probabilistic Methods in Quantum Field Theory and Quantum Gravity*, Proceedings of the NATO Advanced Study Institute, Cargese, France, 1989, edited by P. H. Damgaard *et al.*, NATO ASI Series B: Physics Vol. Vol. 224 (Plenum, New York, 1990), and references therein.
- [12] J.E. Mandula and M. Ogilvie, *Phys. Lett. B* **185**, 127 (1987).
- [13] D. Zwanziger, *Phys. Lett. B* **257**, 168 (1991).
- [14] E. Marinari, C. Parrinello, and R. Ricci, *Nucl. Phys.* **B362**, 487 (1991).
- [15] R. Gupta, G. Guralnik, G. Kilcup, A. Patel, S. Scharpe, and T. Warnock, *Phys. Rev. D* **36**, 2813 (1987).
- [16] C. Bernard, A. Soni, and K. Yee, in *Lattice '90*, Proceedings of the International Symposium, Tallahassee, Florida, 1990, edited by U. M. Heller, A. D. Kennedy, and S. Sanielevici [Nucl. Phys. B (Proc. Suppl) **20**, 410 (1991)].
- [17] C. Bernard, *Phys. Lett.* **108B**, 432 (1982); *Nucl. Phys.*



- B219**, 341 (1983).
- [18] See the Appendix of S. Gottlieb *et al.*, Nucl. Phys. **B263**, 704 (1986).
- [19] C. Bernard, J. Labrenz, and A. Soni, Phys. Rev. D (to be published); in *Lattice '92*, Proceedings of the International Symposium, Amsterdam, The Netherlands, 1992, edited by J. Smit and P. van Baal [Nucl. Phys. B (Proc. Suppl.) **30**, 465 (1993)].
- [20] See, for instance, D. Toussaint, in *From Actions to Answers*, Proceedings of the Theoretical Advanced Study Institute in Elementary Particle Physics, Boulder, Colorado, 1989, edited by T. DeGrand and D. Toussaint (World Scientific, Singapore, 1990), p. 121.
- [21] M. L. Paciello *et al.*, Phys. Lett. B **289**, 405 (1992).
- [22] D. Zwanziger, "Fundamental Modular Region, Boltzmann Factor and Area Law in Lattice Gauge Theory," Report No. NYU-TP-9351 (unpublished).